Vol. **114** (2008) *ACTA PHYSICA POLONICA A* No. 4

Raman Scattering and Electrical Properties of TGS:PCo (9%) Crystal as Ambient Temperature IR Detector

R. Malekfar* and A. Daraei

Physics Department, Faculty of Basic Sciences, Tarbiat Modares University
P.O. Box 14115-175, Tehran, I.R. Iran

(Received May 8, 2008)

We developed and adequately characterized the triglycine sulfate family crystals doped with specific molar percent of cobalt phosphate, TGS:PCo (9%). The crystals were grown by slow evaporation technique and the growth rates of different crystallographic planes are rather faster in comparison with the plane growth rates of pure TGS crystals. The introduction of Co^{2+} ion as an active optical element to the structure of TGS crystal leads to optimization of some parameters such as optical quality, stability at ambient condition, Curie temperature, stronger Raman peaks, etc. Three new peaks at 460, 620 and 1368 cm^{-1} were observed in the dispersive back scattering Raman spectra of the grown TGS:PCo (9%) crystal in comparison with the pure triglycine sulfate crystal.

PACS numbers: 78.30.–j, 77.84.Fa

1. Introduction

Triglycine sulphate (TGS for short) crystals with the chemical formula $(NH_2CH_2COOH)_3 \cdot H_2SO_4$ exhibit good pyroelectric properties and find wide applications as infrared pyroelectric detectors in environmental analysis monitors, earth observation cameras, astronomical telescopes, military systems and target faces vidicons [1]. TGS undergoes a second-order ferroelectric phase transition at the Curie point $T_c = 49°C$. It belongs to the monoclinic system both in the ferroelectric and paraelectric phases. Below T_c, it belongs to the polar point group 2 with the spontaneous polarization along the b-axis. In the paraelectric phase the crystal belongs to the centro-symmetric point group $2/m$ [2]. They are ferroelectric crystals, which have a maximum pyroelectric sensitivity at room temperature and therefore do not require the cooling for detection of temperature changes and exhibit a large spontaneous electrical polarization below T_c. However, the main

*corresponding author; e-mail: Malekfar@Modares.ac.ir

disadvantages of the TGS crystals are (i) depolarization with time or by thermal, electrical or mechanical means, (ii) hygroscopic and (iii) low Curie temperature [3, 4]. But these can be overcome by suitably substituting the site of glycine by an optically active molecule. Many authors have investigated the effect of various doping on TGS [2–8]. In this research the TGS crystal is doped with a specific percent of $Co_3(PO_4)_2 \cdot 8H_2O$. The introduced Co^{2+} ion produces with glycine chelate complexes which can affect dielectric and pyroelectric properties of the crystal which are important for infrared detectors. In this article we describe the crystal growth process, investigate and measure some specific parameters by using the hysteresis loops and at the end the dispersive backscattering Raman spectroscopy spectra and their assignment will be reported.

2. Experimental procedure

2.1. Crystal growth

Crystals were grown in liquid phase from saturated aqueous solutions with the following chemical compositions in our crystal growth laboratory:

$$3(NH_2CH_2COOH) + H_2SO_4 \rightarrow \text{TGS},$$

$$3(NH_2CH_2COOH) + 0.91H_2SO_4 + 0.09[Co_3(PO_4)_2 \cdot 8H_2O] \rightarrow \text{TGS} : \text{PCo}(9\%).$$

The crystals were grown using the hung rotating seed in growth solutions with decreasing temperature. The seed being hung into the growth solution was connected to a rotator which was rotating with a fixed velocity of 1 rpm. The rotator and growth solution were placed in an almost insulated box and then the box was fixed in a temperature controlled room. The outside box temperature decreased from 50°C to 38°C in a time interval of 15 to 20 days and suitable crystals were obtained after this period of time. Figure 1 shows typical as-grown

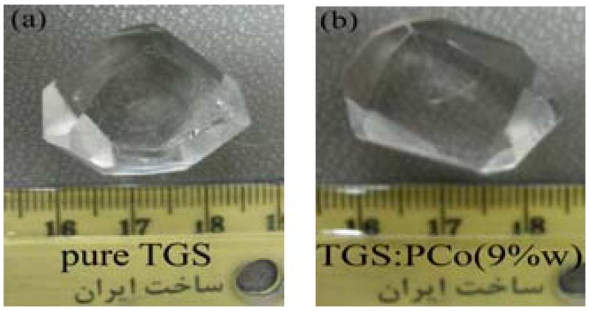

Fig. 1. The grown crystals: (a) pure TGS crystal and (b) TGS:PCo(9%) crystal.

sample crystals of pure TGS and TGS:PCo(9%). As-grown doped sample crystals had better optical quality from optical transparency point of view, in comparison with the pure crystal samples. We have also found that in the growth processes

the quality of growth at a, b and c crystallographic directions are similar for both pure and doped samples, but the doped crystals grow much faster in comparison with the pure crystals.

2.2. Samples preparation

The best grown pure and doped crystals from optical transparency point of view were selected and different crystallographic planes were assigned. An example of the different crystal planes in TGS family of crystals has been schematically shown in Fig. 2. Since the ferroelectric crystallographic axis is b, so for studying the

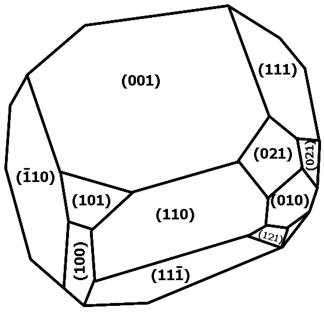

Fig. 2. Typical morphology of a naturally grown crystal of TGS.

ferroelectric character and also the Raman spectroscopy of this family of crystals the measurements should be performed in this direction. Therefore we grow pure and doped crystals with a large (010) planes and cut all the crystals along the b crystallographic axis. The crystals cutting process was done using a sharp blade and then samples were polished to make them ready for studying. The typical sizes of samples were about 1.9–2 mm in thickness and 120 mm^2 large in area [9].

3. Results and discussions

3.1. P–E hysteresis loop

The Sawyer–Tower circuit was used to measure the hysteresis loop (Fig. 3a). A hysteresis loop similar to $P-E$ hysteresis loop can be seen on the oscilloscope screen (Fig. 3b). The oscilloscope registers the V_0 and V_1 voltages. Since we are using an ac voltage along with a capacitor (C_1) then the difference between the voltages appear as hysteresis loop.

The dependence of $P-E$ hysteresis loop on the V_1-V_0 hysteresis loop or the relation among the polarization and electric field and V_0 and V_1 voltages is

$$E = \frac{V_0 - V_1}{d}, \tag{1}$$

$$P = \frac{C_1}{A} V_1 - \varepsilon_0 \frac{V_0 - V_1}{d}, \tag{2}$$

where A and d are the thickness and the area of the sample, respectively.

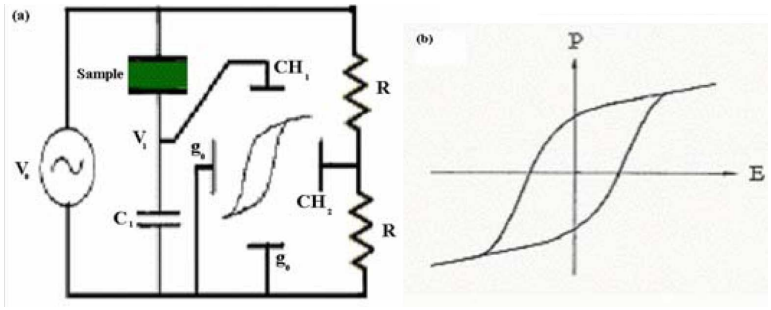

Fig. 3. (a) Sawyer–Tower circuit for measuring the hysteresis loop. (b) $P-E$ hysteresis loop.

ε_0 is the dielectric constant of free space (8.85×10^{-12} C^2/(N m^2)) and C_1 is the capacity [10].

In order to increase the temperature range the capacitor was attached to the mercury region of a thermometer in a laboratory tube and all of them placed in a large container kept at 0°C temperature. The first hysteresis loop was observed at this temperature, then in the next step by using a heater we increased the temperature of the assembly and took photos from the changes in the hysteresis loop on the screen of the oscilloscope. We continued the increase in the temperature of the assembly until the hysteresis loop went into a line. The temperature at which the hysteresis loop becomes a line is the Curie temperature of the crystal. At temperatures higher than the Curie temperature, the results between the polarization and the electric field behave in a linear relationship. According to Eq. (2) when V_1 becomes zero this kind of effects can be seen. Then the polarization only depends on the second term of Eq. (2) (the applied field) and P and E will have a

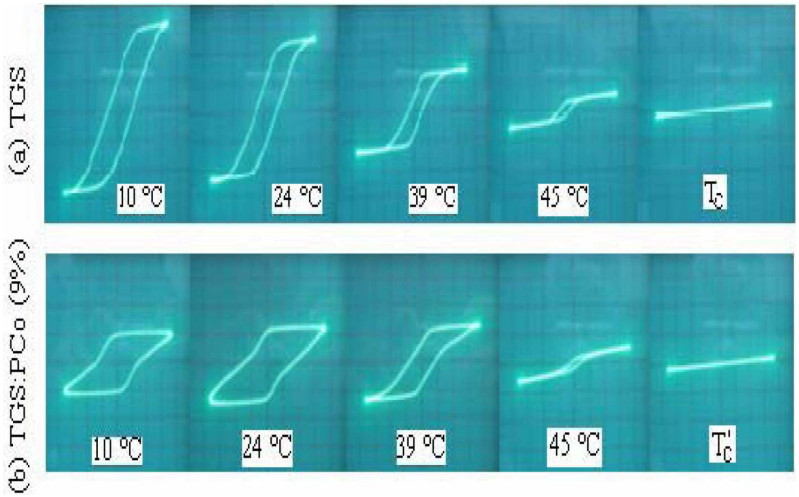

Fig. 4. Measured hysteresis loops in various temperatures for: (a) pure TGS, (b) TGS:PCo(9%).

linear relationship. By following this method the Curie temperature of the grown crystals can be calculated. Figure 4 shows the hysteresis loops for pure TGS and TGS:PCo(9%) samples at various temperatures.

As can be seen from Fig. 4 the hysteresis loop in doped samples has a double form. This can be a consequence of the PO_4^{3-} ions [11].

¿From the hysteresis loop on the screen and Eqs. (1) and (2) we can calculate the remanent polarization P_r and coercive field E_c. So by having the hysteresis loops at different temperatures we can determine the temperature dependence of P_r and E_c. By plotting P_r and E_c for TGS:PCo(9%) sample versus temperature, we can see that they are very similar to those of pure TGS sample (see Fig. 5 and Ref. [12]).

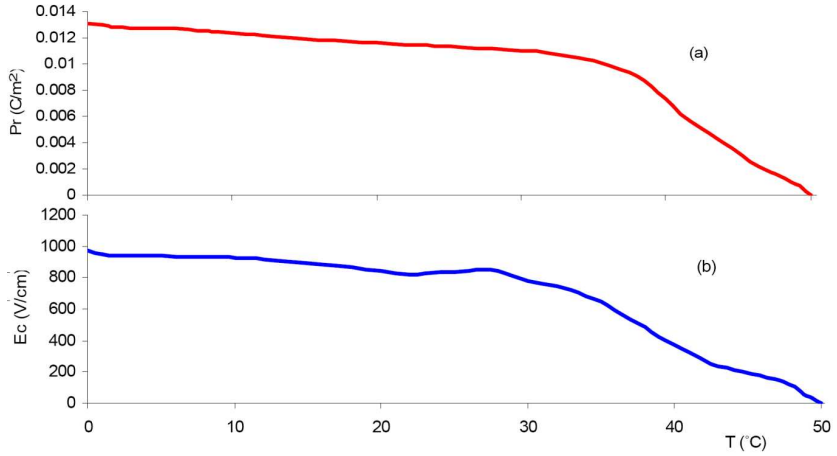

Fig. 5. Physical parameters of TGS:PCo(9%): (a) remanent polarization and (b) coercive field.

¿From the graphs in Fig. 5 the exact values of P_r and E_c at room temperature can be calculated and also it is possible to calculate the Curie temperature of the samples (Table I).

TABLE I

Measured parameters from the hysteresis loops for pure TGS and TGS:PCo(9%) crystals.

Sample	TGS	TGS:PCo(9%)
T_c [°C]	49.5	50
P_r [μC/m^2] at room temperature	4900	13000
E_c [V/cm] at room temperature	330	972

By investigating the Curie temperatures of the pure and doped samples, we can find an increase in the Curie temperature of the doped crystal in comparison with the pure TGS crystal, which can be an advantage for the doped crystal sample. P_r and E_c of the doped sample are larger than that in comparison with

pure TGS sample. This is due to the presence of Co^{2+} ions in the doped TGS crystal structure. Since the Co^{2+} ions are more polar, they increase the sample polarization and in turn can resist the applied external electric field. In this case the required applied field for aligning the doped samples must be larger than that for the pure TGS crystal.

3.2. Raman scattering spectroscopy

Raman spectroscopy for the pure and doped samples was performed along the *b* crystallographic direction and for the (010) plane at room temperature using a Thermo Nicolet Almega Dispersive Raman spectrometer equipped with a second harmonic 532 nm laser line in a backscattering configuration. Typical Raman spectra are presented in Figs. 6 and 7. The Raman spectra were recorded in the spectral region 75–4250 cm^{-1}. We observed no peaks in the region 1800–2200 cm^{-1}. Accordingly we separate the recorded spectra in two different regions

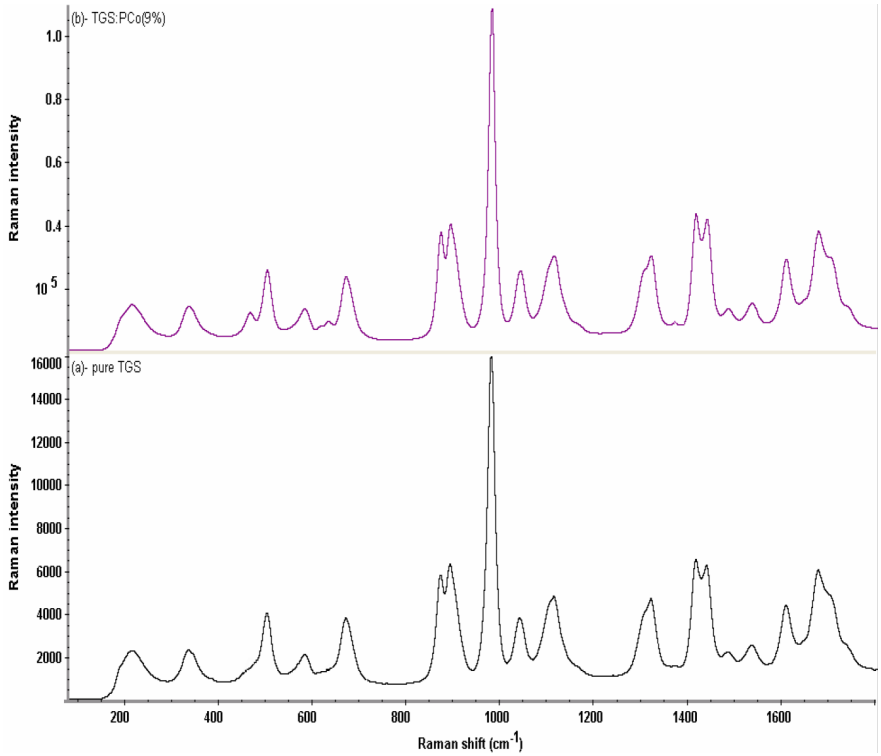

Fig. 6. Typical Raman spectra of the grown (a) pure TGS and (b) TGS:PCo(9%) crystals with the Raman intensity against the Raman shift in the spectral region of 75–1800 cm^{-1}.

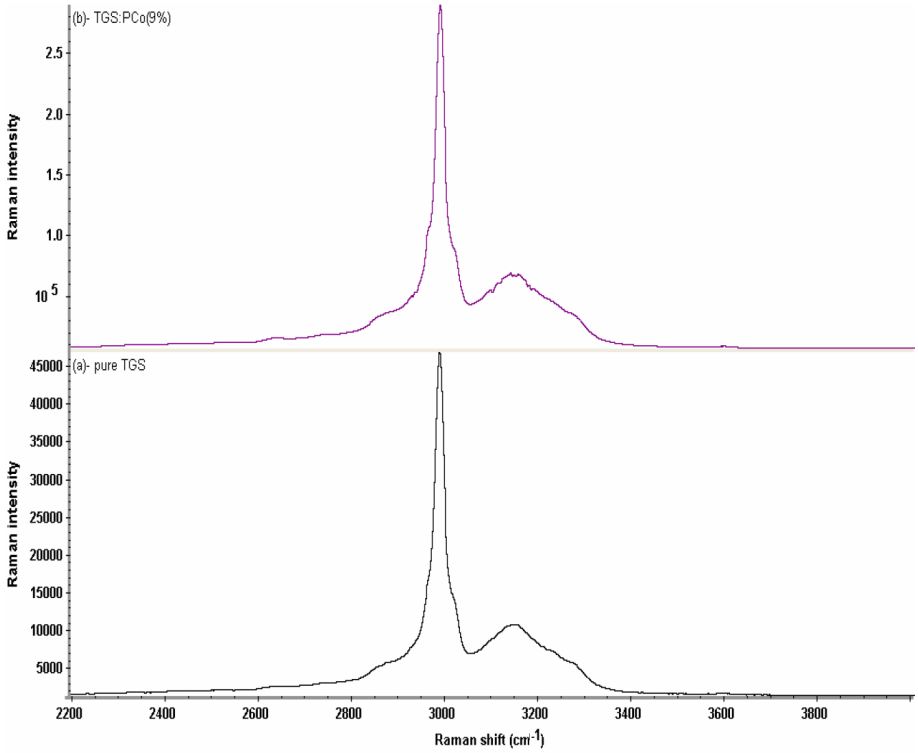

Fig. 7. Typical Raman spectra of the grown (a) pure TGS and (b) TGS:PCo(9%) crystals with the Raman intensity against the Raman shift in the spectral region of 2200–4000 cm^{-1}.

i.e. 75–1800 cm^{-1} and 2200–4000 cm^{-1} as typically have been shown in Figs. 6 and 7, respectively.

The experimental Raman spectroscopy parameters such as laser intensity, resolution, number of scans, slit widths, etc. are similar for both samples. However, due to the good optical transparency of the doped crystal and as can be seen from the Raman intensities of the spectra in the figures the Raman intensity of the doped sample is about 6.5–7 times more intense than that for pure TGS. This can prove that the doped sample has much better optical quality.

By using the literature reported Raman spectral data of SO_4, CH_2, NH_3 and C–H groups and also by comparing the recorded Raman spectra we assigned the observed Raman lines which have been summarized in Table II. In comparison with pure TGS crystal, three peaks at 460 cm^{-1}, 620 cm^{-1} and 1368 cm^{-1} are observed for TGS:PCo(9%) crystal.

The observed Raman lines are compared with those cited in the literature and references. Most of our assignments agree with previously reported values [9, 13, 14].

TABLE II

Characteristic Raman modes of the peaks in Raman spectra of the samples.

Mode	TGS [cm^{-1}]	TGS:PCo (9%) [cm^{-1}]
CO_2 torsion	209	209
glycine	331	331
SO_4		460
C–CO bending	498	498
C–CO bending	578	578
SO_4		620
O–C–O bending	666	667
C–C stretching	868	870
C–C stretching	889	890
SO_4	976	978
SO_4	1037	1039
NH_3 rocking	1110	1111
CH_2 wagg/twist	1318	1318
CH_2 wagg/twist		1368
CO_2 symmetric stretch mode	1414	1414
CH_2 bending	1436	1437
CH_2 scissoring	1484	1482
NH_3	1533	1534
NH_3	1607	1607
C=O	1675	1676
CH_2 stretching	2983	2985
NH_2 stretching	3146	3150

4. Conclusions

In order to overcome the problems and to optimize the optical properties of TGS family of crystals, we have reported the process of the growth of doped TGS crystal with 9% mole of cobalt phosphate hydrate as dopant. The growth rates at different planes were faster for the doped crystal in comparison with the pure TGS crystal. We have also found that the doped crystal has grown with better optical transparency which is obvious from the more intense Raman spectrum of the doped sample. By using the Sawyer–Tower circuit, we have recorded the hysteresis loops at different temperatures and have determined the temperature dependence of the remanent polarization, P_r, and the coercive field, E_c, for the pure and doped grown crystals. The Curie temperature and also the values of P_r and E_c of the doped crystals have increased. By recording the Raman spectra at

room temperature three extra peaks at 460 cm^{-1}, 620 cm^{-1} and 1368 cm^{-1} are observed for doped crystal in comparison with the pure sample.

References

[1] V.V. Emov, V.V. Ivanov, E.A. Klevzova, N.N. Novikova, V.V. Sikolenko, S.I. Tiutunnikov, E.A. Vinogradov, V.A. Yakovlev, *Particles Nuclei Lett.* **115**, 65 (2002).

[2] G. Arunmozhi, S. Lanceros-Mendez, E. de Matos Gomes, *Mater. Lett.* **54**, 329 (2002).

[3] S. Satapathy, S.K. Sharma, A.K. Karnal, V.K. Wadhawan, *J. Cryst. Growth* **240**, 196 (2002).

[4] K. Meera, R. Muralidharan, A.K. Tripathi, P. Ramasamy, *J. Cryst. Growth* **263**, 524 (2004).

[5] R. Muralidharan, R. Mohankumar, R. Dhanasekaran, A.K. Tirupathi, R. Jayavel, P. Ramasamy, *Mater. Lett.* **57**, 3291 (2003).

[6] L. Prokopova, J. Novotny, Z. Micka, V. Malina, *Cryst. Res. Technol.* **36**, 1189 (2001).

[7] B.J. Lillicrap, J.D.C. Wood, V.M. Wood, N. Shaw, *J. Phys. D, Appl. Phys.* **12**, 633 (1979).

[8] J. Novotny, L. Prokopova, Z. Micka, *J. Cryst. Growth* **226**, 333 (2001).

[9] E.M. Mihaylova, H.J. Byrne, *J. Phys. Chem. Solids* **61**, 1919 (2002).

[10] M.M. Berkens, Th. Kwaaitaal, *J. Phys. E, Sci. Instrum.* **16**, 516 (1983).

[11] A. Saxena, M. Fahim, V. Gupta, K. Sreenivas, *J. Phys. D, Appl. Phys.* **36**, 3168 (2003).

[12] B. Fugiel, *Pergamon Solid State Commun.* **122**, 237 (2002).

[13] C. Murli, S.M. Sharma, S. Karmakar, S.K. Sikka, *Physica B* **339**, 23 (2003).

[14] G. Socrates, *Infrared and Raman Characteristic Group Frequencies*, 3rd ed., Wiley, New York 2004, p. 347.